Ann. of Appl. Math.
33:1(2017), 6-17

LOCALIZED PATTERNS OF THE SWIFT-HOHENBERG EQUATION WITH A DISSIPATIVE TERM[*]

Yongli Liu, Yancong Xu[‡]

(*Dept. of Math., Hangzhou Normal University, Hangzhou 310036, Zhejiang, PR China*)

Abstract

In this paper, the normal form analysis of quadratic-cubic Swift-Hohenberg equation with a dissipative term is investigated by using the multiple-scale method. In addition, we obtain Hamiltonian-Hopf bifurcations of two equilibria and homoclinic snaking bifurcations of one-peak and two-peak homoclinic solutions by numerical simulations.

Keywords bifurcation; normal form; Swift-Hohenberg equation; Hamiltonian-Hopf; snakes

2000 Mathematics Subject Classification 35B32

1 Introduction

Spatially localized patterns are associated with particular stationary solutions of mathematical models described by partial differential equations, such as the Swift-Hohenberg equation and Ginzburg-Landau equation. These patterns have also been observed in many bistable systems and investigated intensively [1-22], particularly the localised roll patterns, which correspond to homoclinic orbits of the associated ordinary differential equations. For example, homoclinic snaking curve, see Figure 1 for details, has been observed in many reversible hamiltonian systems, here homoclinic snaking refers to a branch curve of homoclinic orbits near a heteroclinic cycle with the increasing width of localized rolls.

Consider the following Swift-Hohenberg equation

$$u_t = -\mu u - (1+\partial_x^2)^2 u + bu^2 - u^3, \quad x \in R. \tag{1}$$

It is easy to see that if we treat μ as a bifurcation parameter, then at $\mu = 0$, the bifurcation is subcritical if $b^2 > \frac{27}{38}$ and supercritical if $b^2 < \frac{27}{38}$. Furthermore, equa-

[*]This project was supported by the National NSF of China (Nos.11671114 and 11571088) and Program for Excellent Young Teachers in HNU (HNUEYT2013).

[†]Manuscript received August 24, 2016; Revised October 20, 2016

[‡]Corresponding author. E-mail: yancongx@163.com

tion (1) with $u_t = 0$ is a reversible and conservative system, which has the first integral

$$H_1(u) = \frac{1}{2}(\mu+1)u^2 + u_x^2 - \frac{1}{2}u_{xx}^2 + u_x u_{xxx} + \frac{1}{3}bu^3 - \frac{1}{4}u^4. \tag{2}$$

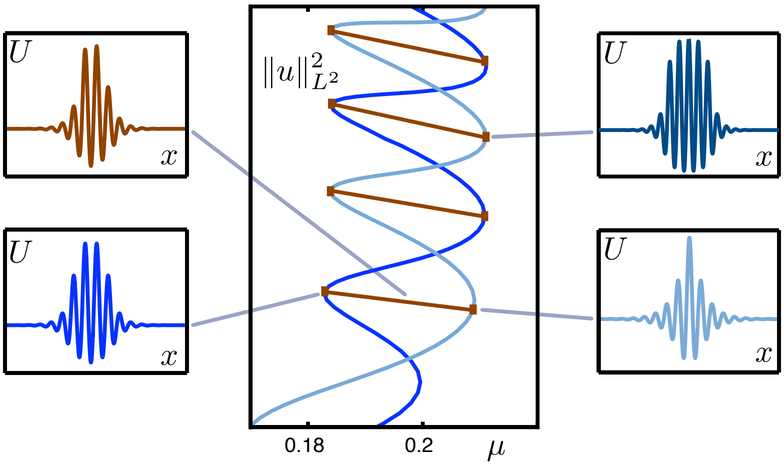

Figure 1: Homoclinic snaking curve

Figure 1 shows snaking bifurcation of symmetric solutions, laddering bifurcation of non-symmetric solutions and four sample solution profiles of Swift-Hohenberg equation (1). Also the brown solution profile is non-symmetric, each of the baby blue solution profiles is symmetric with a maximum and the blue solution profile is symmetric with a minimum.

Burke et al. [2] studied a modified Swift-Hohenberg equation

$$u_t = -\mu u - (1+\partial_x^2)^2 u + bu^2 - u^3 + \gamma u_{xxx} \tag{3}$$

with $b = 2$, which is a perturbation of (1) with a dissipative term γu_{xxx}, which destroy both the reversibility symmetry and variational property. As suggested by the authors that the snakes and ladders structure had been broken into a stack of isolas rather than snakes. Knobloch et al. [10] proved the existence of the isolas of 2-pulse solutions about stationary 1D patterns of the normal quadratic-cubic Swift-Hohenberg equation.

In this paper, we consider a Swift-Hohenberg equation with a non-reversible and conservative term, which also presents the existence of one-pulse and two-pulse snakes with a stack of saddle-nodes rather than a stack of pitch-forks. More precisely, we consider the normal form and bifurcation of the following perturbed Swift-Hohenberg equation with a dissipative term

$$u_t = -\mu u - (1+\partial_x^2)^2 u + bu^2 - u^3 + \alpha u_x u_{xx}, \tag{4}$$

which is a variational and non-reversible system when $\alpha \neq 0$. We use both μ and b

as bifurcation parameters, but μ is used as the primary control parameter. Note that, generally equation (4) can be rewritten into an ordinary differential equation

$$-\mu u-(1+\partial_x^2)u+b_2u^2+u^3+\alpha\partial_x u\partial_{xx}u=0. \tag{5}$$

Also it is easy to see that equation (4) is a variational system satisfying

$$u_t=-\frac{\delta F}{\delta u}, \tag{6}$$

where the Lyapunov function $F[u(x,t)]$ is as follows

$$F=\int_{-\infty}^{+\infty}\mathrm{d}x\Big[\frac{1}{2}\mu u^2+\frac{1}{2}\big((1+\partial_x^2)^2u\big)^2-\frac{1}{3}bu^3+\frac{1}{4}u^4-\frac{1}{2}\alpha(u_xu_{xx})^2\Big]. \tag{7}$$

One can verify that

$$\frac{\mathrm{d}F}{\mathrm{d}t}=-\Big(\frac{\partial u}{\partial t}\Big)^2\le 0, \tag{8}$$

which implies that F is non-increasing in t. Thus in a finite domain with null boundary conditions all solutions evolve towards stationary states; in an unbounded domain or periodic domain solutions in the form of moving fronts are possible. If we regard function $F[u]$ as the free energy of the system, then the stable and unstable solutions corresponds to the local minima and local maxima of F, respectively.

Linearise (4) at $u=0$ and consider a solution of the form $u\propto\exp(\sigma_k t+ikx)$, where σ_k is the growth rate of a perturbation with wavenumber k. Then σ_k is determined by the dispersion relation

$$\sigma_k=-\mu-(1-k^2)^2. \tag{9}$$

Setting $\sigma_k=0$ yields the marginal stability curve, and then minimising the marginal value $\mu=\mu_k$ about wavenumber k leads to the prediction $\mu=0$ for the onset of instability, about the associated wavenumber, $k=1$. Observe that if one takes $\mu>0$ then the condition for marginal stability, $\mu=-(1-k^2)^2$, has no solution for real k; however, when $\mu<0$, there is a pair of real solutions, $k=k_\pm$ with $k_-<1<k_+$. As magnitude of μ decreases to zero, wavenumbers $k_\pm$ approach $k=1$ from opposite directions and at $\mu=0$ they collide at $k=1$. Thus the minimum of the marginal stability curve is in fact associated with the collision of two roots of the marginal dispersion relation.

In addition, if we focus on the dynamics of steady state solutions in equation (4), satisfying

$$-\mu u-\Big(1+\frac{\mathrm{d}^2}{\mathrm{d}x^2}\Big)^2u+bu^2-u^3+\alpha u_xu_{xx}=0, \tag{10}$$

we study the stability of the trivial state $u=0$ in space by linearizing (10) around $u=0$ and looking for solutions of the form $u\propto\exp(\lambda x)$, then we have

$$(1+\lambda^2)^2+\mu=0. \tag{11}$$

For $\mu > 0$ the spatial eigenvalues of $u = 0$ are $\lambda^2 = -1 \pm \sqrt{\mu}\, i$, which means that there are two pairs of conjugate complex eigenvalues. At $\mu = 0$ these eigenvalues are $\lambda = \pm i$ (double), which collide pairwise on the imaginary axis for $\mu < 0$ and $|\mu|$ is small enough, then $\lambda^2 = -1 \pm \sqrt{-\mu}$, they split but remain on the imaginary axis, which is so-called Hamiltonian-Hopf bifurcation. The presence of a Hamiltonian-Hopf bifurcation is usually detected by computing the eigenvalue behavior of the linearized system at the bifurcation value of the parameter the system depends upon. The eigenvalues change from purely imaginary to eigenvalues with non-zero real part.

Obviously, the temporal and spatial points of view are closely related; in particular, the onset of instability in the temporal point of view is equivalent to the presence of a pair of purely imaginary spatial eigenvalues of double multiplicity.

Check the transition at $\mu = 0$ in details. Define $\mu = \epsilon^2 \tilde{\mu}$, where $\tilde{\mu} = O(1)$ and $\epsilon \ll 1$. By Taylor expansion, we then find that the spatial eigenvalues are $\lambda = \pm\frac{1}{2}\epsilon\sqrt{\tilde{\mu}} \pm i(1+O(\epsilon^2))$ if $\tilde{\mu} > 0$, while the eigenvalues are $\lambda = \pm\frac{1}{2}\epsilon\sqrt{-\tilde{\mu}} \pm i(1+O(\epsilon^2))$ if $\tilde{\mu} < 0$. These conditions suggest that when $\mu > 0$ the solutions near $u = 0$ increase or decay exponentially as $u \sim \exp(\pm\epsilon\sqrt{-\tilde{\mu}}x/2)$.

If $\alpha \neq 0$, then it is a non-reversible and conservative system, it still has the snaking bifurcation of one-pulse, but the loss of reversibility destroys the pitch-fork bifurcation responsible for the rung bifurcation into a saddle-node bifurcation. It was proved in [12] and [19]. Note that, when we carry out the numerical simulations by AUTO [7], the two-pulse solutions of the snaking curve are varied from a periodic solution to another periodic solution during their drifts, however, the width of the roll patterns becomes wider and wider until they goes to ∞, which means that they become periodic solutions.

The remainder of this paper is organized as follows: In the next section we outline the normal form analysis of (4) by using the multi-scale method. In Section 3, we give Hopf bifurcations of two equilibria and the bifurcation diagram of one-pulse and two-pulse. Finally, we draw some conclusions and outlook.

2 Normal Form Analysis

If we define $u(x,t) = \tilde{u}(x-ct,t) = \tilde{u}(z,t)$, where c is the velocity of wave, then substituting this into equation (4), still denoting by u, it follows that

$$u_t = -\mu u - (1+\partial_z^2)^2 u + bu^2 - u^3 + \alpha u_z u_{zz} + c u_z. \tag{12}$$

By expanding $u(z,t)$ as a sum of Fourier modes multiplied by amplitudes that depends on spatial and temporal scales, we introduce a small parameter $\varepsilon \ll 1$ and rescale the parameters as

$$\mu = \varepsilon^4 \hat{\mu}, \quad b = b_0 + \varepsilon^2 \hat{b}, \quad \alpha = \alpha_0 + \varepsilon^2 \hat{\alpha}, \quad c = \varepsilon^4 \hat{c}, \tag{13}$$

where b_0, α_0 are the values of the quadratic and the cubic coefficients corresponding to $q_1 = 0$, and $\hat{\mu}, \hat{b}, \hat{\alpha}$ are all $O(1)$. Next, we define the large spatial scale $Z = \varepsilon^2 z$ and long time scale $T = \varepsilon^4 t$, and propose the following ansatz for solutions of (12):

$$u(z,t) = \varepsilon^2\Theta + [\varepsilon A\mathrm{e}^{iz} + \varepsilon^2 B\mathrm{e}^{2iz} + \varepsilon^3 C\mathrm{e}^{3iz} + \varepsilon^4 D\mathrm{e}^{4iz} + c.c.] + O(\varepsilon^5), \tag{14}$$

where Θ, A, B, C, D are functions of Z and T, which are all $O(1)$, the higher order terms in ε take the form $\varepsilon_n \mathrm{e}^{niz} + c.c.$ for $n \geqq 5$, and "*c.c.*" denotes complex conjugation of the terms preceding it within the brackets.

Putting the change into (12), we have

$$\begin{aligned}
u_t &= -\mu u - (1+\partial_z^2)^2 u + bu^2 - u^3 + \alpha u_z u_{zz} + cu_z \\
&= -(\varepsilon^4\hat{\mu}+1)[\varepsilon^2\Theta+\varepsilon A\mathrm{e}^{iz}+\varepsilon^2 B\mathrm{e}^{2iz}+\varepsilon^3 C\mathrm{e}^{3iz}+\varepsilon^4 D\mathrm{e}^{4iz}+\varepsilon\bar{A}\mathrm{e}^{-iz}+\varepsilon^2\bar{B}\mathrm{e}^{-2iz} \\
&\quad +\varepsilon^3\bar{C}\mathrm{e}^{-3iz}+\varepsilon^4\bar{D}\mathrm{e}^{-4iz}] - 2\partial_z^2[\varepsilon^2\Theta+\varepsilon A\mathrm{e}^{iz}+\varepsilon^2 B\mathrm{e}^{2iz}+\varepsilon^3 C\mathrm{e}^{3iz}+\varepsilon^4 D\mathrm{e}^{4iz} \\
&\quad +\varepsilon\bar{A}\mathrm{e}^{-iz}+\varepsilon^2\bar{B}\mathrm{e}^{-2iz}+\varepsilon^3\bar{C}\mathrm{e}^{-3iz}+\varepsilon^4\bar{D}\mathrm{e}^{-4iz}] - \partial_z^4[\varepsilon^2\Theta+\varepsilon A\mathrm{e}^{iz}+\varepsilon^2 B\mathrm{e}^{2iz} \\
&\quad +\varepsilon^3 C\mathrm{e}^{3iz}+\varepsilon^4 D\mathrm{e}^{4iz}+\varepsilon\bar{A}\mathrm{e}^{-iz}+\varepsilon^2\bar{B}\mathrm{e}^{-2iz}+\varepsilon^3\bar{C}\mathrm{e}^{-3iz}+\varepsilon^4\bar{D}\mathrm{e}^{-4iz}]+(b_0+\varepsilon^2\hat{b})[\varepsilon^2\Theta \\
&\quad +\varepsilon A\mathrm{e}^{iz}+\varepsilon^2 B\mathrm{e}^{2iz}+\varepsilon^3 C\mathrm{e}^{3iz}+\varepsilon^4 D\mathrm{e}^{4iz}+\varepsilon\bar{A}\mathrm{e}^{-iz}+\varepsilon^2\bar{B}\mathrm{e}^{-2iz}+\varepsilon^3\bar{C}\mathrm{e}^{-3iz}+\varepsilon^4\bar{D}\mathrm{e}^{-4iz}] \\
&\quad \cdot[\varepsilon^2\Theta+\varepsilon A\mathrm{e}^{iz}+\varepsilon^2 B\mathrm{e}^{2iz}+\varepsilon^3 C\mathrm{e}^{3iz}+\varepsilon^4 D\mathrm{e}^{4iz}+\varepsilon\bar{A}\mathrm{e}^{-iz}+\varepsilon^2\bar{B}\mathrm{e}^{-2iz}+\varepsilon^3\bar{C}\mathrm{e}^{-3iz}+\varepsilon^4\bar{D}\mathrm{e}^{-4iz}] \\
&\quad -[\varepsilon^2\Theta+\varepsilon A\mathrm{e}^{iz}+\varepsilon^2 B\mathrm{e}^{2iz}+\varepsilon^3 C\mathrm{e}^{3iz}+\varepsilon^4 D\mathrm{e}^{4iz}+\varepsilon\bar{A}\mathrm{e}^{-iz}+\varepsilon^2\bar{B}\mathrm{e}^{-2iz}+\varepsilon^3\bar{C}\mathrm{e}^{-3iz}+\varepsilon^4\bar{D}\mathrm{e}^{-4iz}] \\
&\quad \cdot[\varepsilon^2\Theta+\varepsilon A\mathrm{e}^{iz}+\varepsilon^2 B\mathrm{e}^{2iz}+\varepsilon^3 C\mathrm{e}^{3iz}+\varepsilon^4 D\mathrm{e}^{4iz}+\varepsilon\bar{A}\mathrm{e}^{-iz}+\varepsilon^2\bar{B}\mathrm{e}^{-2iz}+\varepsilon^3\bar{C}\mathrm{e}^{-3iz}+\varepsilon^4\bar{D}\mathrm{e}^{-4iz}] \\
&\quad \cdot[\varepsilon^2\Theta+\varepsilon A\mathrm{e}^{iz}+\varepsilon^2 B\mathrm{e}^{2iz}+\varepsilon^3 C\mathrm{e}^{3iz}+\varepsilon^4 D\mathrm{e}^{4iz}+\varepsilon\bar{A}\mathrm{e}^{-iz}+\varepsilon^2\bar{B}\mathrm{e}^{-2iz}+\varepsilon^3\bar{C}\mathrm{e}^{-3iz}+\varepsilon^4\bar{D}\mathrm{e}^{-4iz}] \\
&\quad +(\alpha_0+\varepsilon^2\hat{\alpha})\partial_z[\varepsilon^2\Theta+\varepsilon A\mathrm{e}^{iz}+\varepsilon^2 B\mathrm{e}^{2iz}+\varepsilon^3 C\mathrm{e}^{3iz}+\varepsilon^4 D\mathrm{e}^{4iz}+\varepsilon\bar{A}\mathrm{e}^{-iz}+\varepsilon^2\bar{B}\mathrm{e}^{-2iz} \\
&\quad +\varepsilon^3\bar{C}\mathrm{e}^{-3iz}+\varepsilon^4\bar{D}\mathrm{e}^{-4iz}] \cdot \partial_{zz}[\varepsilon^2\Theta+\varepsilon A\mathrm{e}^{iz}+\varepsilon^2 B\mathrm{e}^{2iz}+\varepsilon^3 C\mathrm{e}^{3iz}+\varepsilon^4 D\mathrm{e}^{4iz} \\
&\quad +\varepsilon\bar{A}\mathrm{e}^{-iz}+\varepsilon^2\bar{B}\mathrm{e}^{-2iz}+\varepsilon^3\bar{C}\mathrm{e}^{-3iz}+\varepsilon^4\bar{D}\mathrm{e}^{-4iz}] + \varepsilon^4\hat{c}\partial_z[\varepsilon^2\Theta+\varepsilon A\mathrm{e}^{iz}+\varepsilon^2 B\mathrm{e}^{2iz} \\
&\quad +\varepsilon^3 C\mathrm{e}^{3iz}+\varepsilon^4 D\mathrm{e}^{4iz}+\varepsilon\bar{A}\mathrm{e}^{-iz}+\varepsilon^2\bar{B}\mathrm{e}^{-2iz}+\varepsilon^3\bar{C}\mathrm{e}^{-3iz}+\varepsilon^4\bar{D}\mathrm{e}^{-4iz}].
\end{aligned}$$

After gathering the terms with the same Fourier dependence e^{nix} and keeping careful track, we obtain the following results for $n = 0, 1, 2, 3$ as follows:

$n = 0:$

$$\begin{aligned}
0 = &-\varepsilon^2\Theta + b_0[2\varepsilon^2|A|^2 + \varepsilon^4\Theta^2 + 2\varepsilon^4|B|^2] + 2\varepsilon^4\hat{b}|A|^2 \\
&-3[2\varepsilon^4\Theta|A|^2 + \varepsilon^4\bar{A}^2 B + \varepsilon^4 A^2\bar{B}] + \alpha_0\varepsilon^4(A_Z\bar{A} + A\bar{A}_Z) + O(\varepsilon^6),
\end{aligned} \tag{15}$$

$n = 1:$

$$\begin{aligned}
\varepsilon^5\partial_T A = &-\varepsilon^5\hat{\mu}A + 4\varepsilon^5\partial_{ZZ}A + b_0(2\varepsilon^3\Theta A + 2\varepsilon^3\bar{A}B + 2\varepsilon^5\bar{B}C) \\
&-3(\varepsilon^3 A|A|^2 + \varepsilon^5\Theta^2 A + \varepsilon^5\bar{A}^2 C + 2\varepsilon^5\Theta\bar{A}B + 2\varepsilon^5 A|B|^2) \\
&+\alpha_0(-\varepsilon^5\Theta_Z A + 3\varepsilon^5\bar{A}B_Z + 2i\varepsilon^3\bar{A}B + 6i\varepsilon^5\bar{B}C) \\
&+\hat{\alpha}(i2\varepsilon^5\bar{A}B) + 2\varepsilon^5\hat{b}(\Theta A + \bar{A}B) + \hat{c}i\varepsilon^5 A + O(\varepsilon^7),
\end{aligned} \tag{16}$$

$n=2:$

$$\begin{aligned}0=&-9\varepsilon^2B+24i\varepsilon^4B_Z+b_0(\varepsilon^2A^2+2\varepsilon^4\Theta B+2\varepsilon^4\bar{A}C)\\&-3(\varepsilon^4\Theta A^2+2\varepsilon^4|A|^2B)+\alpha_0(-3\varepsilon^4AA_Z-i\varepsilon^2A^2+i6\varepsilon^4\bar{A}C)\\&-\hat{\alpha}i\varepsilon^4A^2+\hat{b}\varepsilon^4A^2+O(\varepsilon^6),\end{aligned}\tag{17}$$

$n=3:$

$$0=-64\varepsilon^3C+b_0(2\varepsilon^3AB)-\varepsilon^3A^3-\alpha_0(i6\varepsilon^3AB)+O(\varepsilon^5).\tag{18}$$

At first, we need to solve Θ, B, C in terms of the principle amplitude A from (15), (17) and (18). Writing

$$\Theta=\Theta_0+\varepsilon^2\Theta_2+O(\varepsilon^4),\quad B=B_0+\varepsilon^2B_2+O(\varepsilon^4),\quad C=C_0+O(\varepsilon^2),\tag{19}$$

substituting them into (15), (17) and (18), respectively, we obtain the following leading order relations

$$\begin{aligned}&\Theta_0=2b_0|A|^2=c_1|A|^2,\quad B_0=\frac{1}{9}(b_0-i\alpha_0)A^2=c_2A^2,\\&C_0=\frac{1}{64}[2b_0c_2-1-i6\alpha_0c_2]A^3=c_3A^3,\end{aligned}\tag{20}$$

where

$$c_1=2b_0,\quad c_2=\frac{1}{9}(b_0-i\alpha_0),\quad c_3=\frac{1}{64}[2b_0c_2-1-i6\alpha_0c_2].\tag{21}$$

Next, from (15) and (17), we have

$$\Theta_2=\hat{c_1}|A|^2+c_4|A|^4+c_5(\bar{A}A_Z+A\bar{A}_Z),\quad B_2=\hat{c_2}A^2+c_6|A|^2A^2+c_7AA_Z,\tag{22}$$

where

$$\begin{aligned}&\hat{c_1}=2\hat{b},\quad \hat{c_2}=\frac{1}{9}(\hat{b}-\hat{\alpha}i),\\&c_4=[b_0(c_1^2+2|c_2|^2)-3(2c_1+c_2+\bar{c}_2)],\quad c_5=-\alpha_0,\\&c_6=\frac{1}{9}[2b_0c_1c_2+2b_0c_3-3(c_1+2c_2)+c_36\alpha_0i],\quad c_7=\frac{1}{9}(48c_2i-3\alpha_0).\end{aligned}\tag{23}$$

Now let us turn to consider (16), obviously, it contains $O(\varepsilon^3)$ and $O(\varepsilon^5)$ terms. Inserting (22) and (23) into (16), we present $O(\varepsilon^3)$ terms as follows:

$$0=[b_0(2c_1+2c_2)-3+\alpha_02ic_2]A|A|^2.\tag{24}$$

Define

$$q_1\triangleq[b_0(2c_1+2c_2)-3+\alpha_02ic_2].$$

The bracketed quantity determines the criticality of the bifurcation at $\mu=0$. that is,

$$q_1=0,$$

then it follows

$$2\alpha_0^2 + 38b_0^2 = 27.$$

Obviously, its diagram is an ellipse, see Figure 2. Furthermore, if we add another different dissipative term and take a new multiple scale, we can get a hyperbolic curve which reflects the relations of two parameters b_0, α_0.

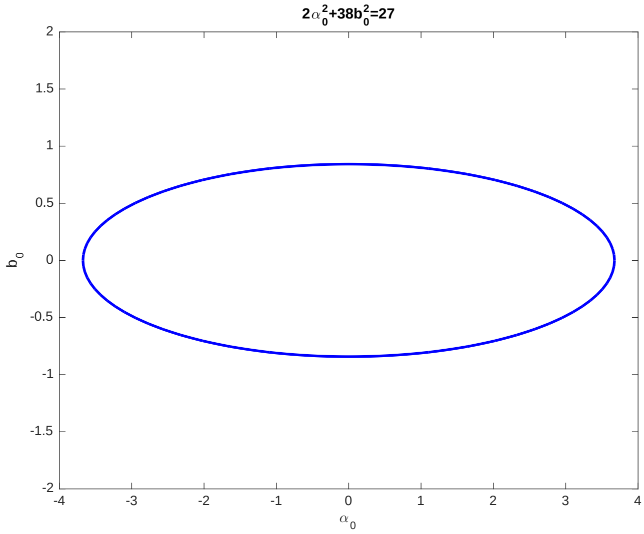

Figure 2: The bifurcation diagram at $\mu = 0$ is an ellipse

Note that, if we take $\alpha_0 = 0$, then the secondary bifurcation parameter b determines the criticality of the pattern-forming instability at $\mu = 0$: it is supercritical if $b^2 < \frac{27}{38}$ and subcritical if $b^2 < \frac{27}{38}$.

The remaining terms are $O(\varepsilon^5)$, and we can obtain a differential equation for the principle amplitude $A(X, T)$:

$$A_T = (-\hat{\mu} + \hat{c}i)A + 4A_{ZZ} + \hat{c}A_Z + c_5 A^2 \bar{A}_Z + c_8|A|^2 A_Z + c_9|A|^2 A + c_{10}|A|^4 A, \quad (25)$$

where

$$\begin{aligned} &c_8 = \alpha_0(\frac{2}{3}\alpha_0 i - \frac{2}{3}b_0 - 1), \quad c_9 = \hat{\alpha}2c_2 i + 2\hat{b}cc_1 + c_2, \\ &c_{10} = 2b_0\bar{c}_2c_3 - 3(c_1^2 + c^3 + 2c_1c_2 + 2|c_2|^2) + 6\alpha_0\bar{c}_2c_3 i, \end{aligned} \quad (26)$$

that is, it is the Ginzburg-Landau approximation of the generalized Swift-Hohenberg equation.

Since we are just concerned about the steady-state solution of equation (4), here we take $\hat{c} = 0$ in (25), then it follows

$$A_T = -\hat{\mu}A + 4A_{ZZ} + c_5 A^2 \bar{A}_Z + c_8|A|^2 A_Z + c_9|A|^2 A + c_{10}|A|^4 A. \quad (27)$$

The time-dependent amplitude equation (27) is the envelope equation to the perturbed Swift-Hohenberg equation (4) valid near onset in the regimes of small criticality, that is, near the codimension-two point $(\mu, q_1) = (0, 0)$. If $\alpha = 0$, the above expressions reduces to the general normal form results for the unperturbed Swift-Hohenberg equation (1).

3 Bifurcation Analysis

In this part, we discuss the Hopf bifurcations of two equilibria and snake bifurcation of homolinic solutions by using AUTO07p.

Since equation (4) is a variational system, all the solutions converge to equilibria and no traveling wave, temporal chaos and sustained oscillations occur. It is also equivariant under the following inversion including parameters: $(x, u; \mu, b, \alpha) \to (x, -u; \mu, -b, \alpha)$.

For steady-state solution of (1), write it to ODE as follows:

$$u_x = f(u, \mu), \quad u = (u_1, u_2, u_3, u_4) = (U, U_x, U_{xx}, U_{xxx}) \in R^4, \tag{28}$$

that is,

$$\dot{u_1} = u_2, \quad \dot{u_2} = u_3, \quad \dot{u_3} = u_4, \quad \dot{u_4} = -(\mu + 1)u_1 - 2u_3 + bu_1^2 - u_1^3 + \alpha u_2 u_3. \tag{29}$$

Now we turn to compute the equilibria of system (29), that is, setting

$$u_2 = 0, \quad u_3 = 0, \quad u_4 = 0, \quad -(\mu + 1)u_1 - 2u_3 + bu_1^2 - u_1^3 + \alpha u_2 u_3 = 0, \tag{30}$$

then we obtain three equilibria

$$E_1(0,0,0,0), \quad E_2\Big(\frac{b - \sqrt{b^2 - 4(\mu+1)}}{2}, 0, 0, 0\Big), \quad E_3\Big(\frac{b + \sqrt{b^2 - 4(\mu+1)}}{2}, 0, 0, 0\Big).$$

According to the above equilibria, we know that the perturbation term $\alpha u_2 u_3$ doesn't change the location and existence of equilibria.

Let us compute the Jacobian matrix of three equilibria of system (29) as follows:

$$Df(u, \mu) = \begin{pmatrix} 0 & 1 & 0 & 0 \\ 0 & 0 & 1 & 0 \\ 0 & 0 & 0 & 1 \\ -\mu - 1 + 2bu_1 - 3u_1^2 & \alpha u_3 & \alpha u_2 - 2 & 0 \end{pmatrix}. \tag{31}$$

At first, we compute the Jacobian matrix of $E_1(0, 0, 0, 0)$, and it follows that

$$Df(0,0,0,0) = \begin{pmatrix} 0 & 1 & 0 & 0 \\ 0 & 0 & 1 & 0 \\ 0 & 0 & 0 & 1 \\ -\mu - 1 & 0 & -2 & 0 \end{pmatrix}, \tag{32}$$

then we get the characteristic equation $\lambda^4 + 2\lambda^2 + \mu + 1 = 0$, which means that $\Lambda \triangleq \lambda^2 = -1 \pm \sqrt{-\mu}$, there are three cases:

(i) For $\mu=0,\ \Lambda=-1$ (double), that is, $\lambda=-i$ (double), $\lambda=i$ (double).

(ii) For $\mu>0,\ \Lambda_1=-1-\sqrt{\mu}i,\ \Lambda_2=-1+\sqrt{\mu}i$, which means that it has two pairs of conjugate complex roots with non-zero real part.

(iii) For $\mu<0,\ \Lambda_1=-1-\sqrt{-\mu}<0$, it follows that $\lambda=\pm\sqrt{1+\sqrt{-\mu}}\ i$ (a pair of pure imaginary roots). While for $\Lambda_2=\lambda^2=-1+\sqrt{-\mu}$, if $\mu=-1$, then $\lambda=0$ (double); if $-1<\mu<0$, then $\lambda=\pm\sqrt{-1+\sqrt{-\mu}}\ \ i$ is a pair of pure imaginary roots; if $\mu<-1$, then $\lambda=\pm\sqrt{\sqrt{-\mu}-1}$ is a pair of real roots. Note that

$$Df\Big(\frac{E_2}{E_3}\Big)=\begin{pmatrix} 0 & 1 & 0 & 0\\ 0 & 0 & 1 & 0\\ 0 & 0 & 0 & 1\\ -\mu-1+b(b\pm\sqrt{b^2-4(\mu+1)})-\frac{3}{4}(b\pm\sqrt{b^2-4(\mu+1)})^2 & 0 & -2 & 0\end{pmatrix}, \tag{33}$$

Define

$$\Omega\triangleq-\mu-1+b(b\pm\sqrt{b^2-4(\mu+1)})-\frac{3}{4}(b\pm\sqrt{b^2-4(\mu+1)})^2,$$

then the corresponding characteristic equation is $\lambda^4-2\lambda^2-\Omega=0$. Due to the complexity of its eigenvalues, here we only consider the special cases. For example, we take $b=1.6$, when $\mu<0.36$, there exist two equilibria E_2, E_3, which means that the system undergoes a pitch-fork bifurcation.

If, for example, we take $\mu=-0.5$, then $E_2(0.8516685,0,0,0)$ and $E_3(1.174657,0,0,0)$. Based on their own Jacobian matrices, it is easy to know that E_2 and E_3 are two saddle-centers.

According to the Jacobian matrix of E_1, it is is easy to obtain that E_1 is a center, and it undergoes a Hopf bifurcation if we carry out numerical simulations, even Torus bifurcations. Then we can continue the system with respect to the primary parameter μ from E_1, and it is easy to find the occurrence of pitch-fork bifurcation and Hopf bifurcation which connects two distinct Hopf points [see, Figure 3, for details], that can also be obtained by using Hopf bifurcation analysis.

Obviously, if $\alpha\neq0$, it is not a reversible system, but it has a Hamiltonian

$$H_2(u)=\frac{\mu+1}{2}u_1^2-u_2^2+\frac{1}{2}u_3^2-u_2u_4+\int_0^{u_1}(bv^2+v^3)\mathrm{d}v+\frac{1}{3}\alpha u_2^3. \tag{34}$$

Now we continue system (29) with the primary parameter μ, then the bifurcation diagram of snakes [Figure 4] and their sample solution profiles [Figure 5] are obtained.

Note that, this kind of non-symmetric snaking curve about one pulse are called "crisis-cross snaking", which has similar situation with the original snake-ladder in Figure 1, the same locations of branch corresponds to non-symmetric solution profiles and symmetric solution profiles except the curve of periodic solution profiles.

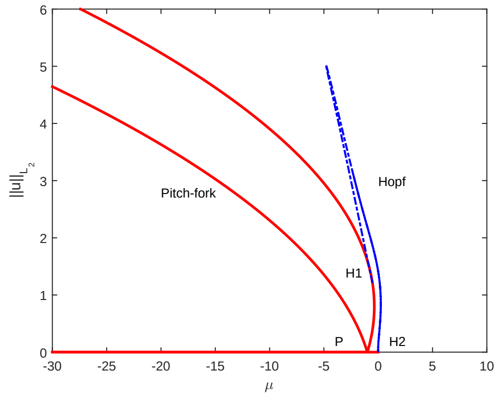

Figure 3: The pitch-fork bifurcation and Hopf bifurcations connect with two Hopf points H_1 and H_2 by continuating from the equilibrium $E_1(0, 0, 0, 0)$ of system (29) when b=1.6, α=0.2.

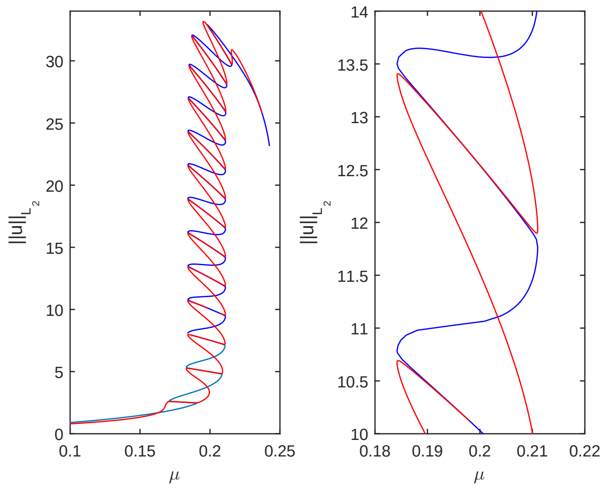

Figure 4: Bifurcation diagram shows two branches of non-symmetric one-pulse localized patterns which emerges from and terminates on the spatially periodic branch as $b = 1.6, \alpha = 0.15$. The second figure is the corresponding part enlarged in the first figure.

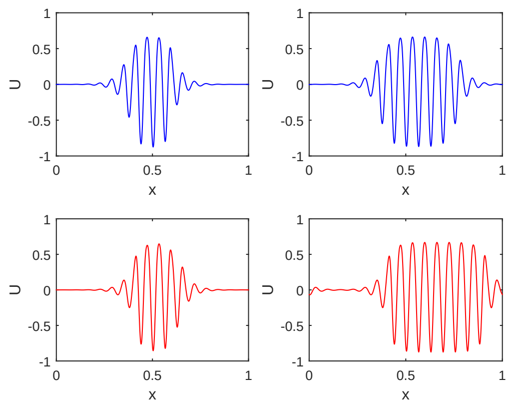

Figure 5: Sample solution profiles of red and blue snaking branches in Figure 4.

Also, the branch curve of two-pulse is continuous as $b = 1.6$, $\alpha = 0.05$. It is easy to see the existence of snakes, then we conclude that the symmetry-breaking terms break the pitchfork branches up into a saddle-node branch and a second branch that does not undergo any bifurcation [Figure 6]. It is natural to put forward to an open problem: Does the bifurcation curve of multi-pulse also present snakes or isolas? Although we can obtain the snake bifurcation of system (29), it is not easy to continue the isola bifurcation.

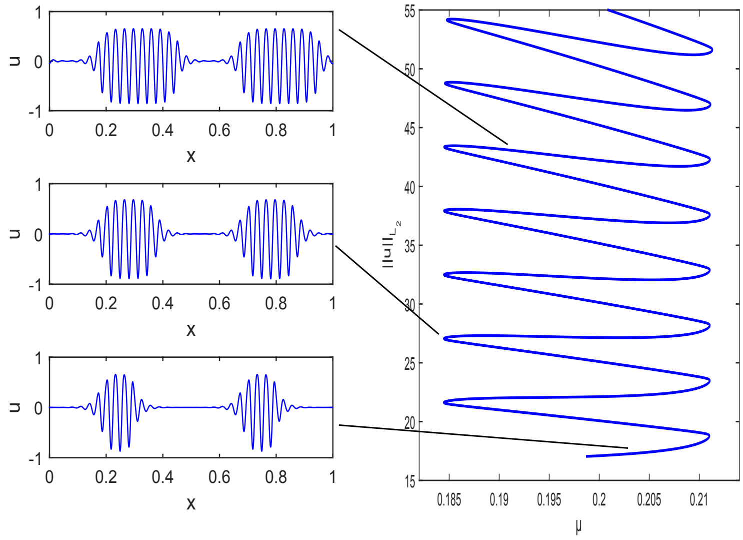

Figure 6: Bifurcation diagram shows snaking curve of non-symmetric two-pulse as the individual width increases when $b = 1.6, \alpha = 0.05$.

4 Conclusions and Discussions

In this paper, we study the effect of non-reversible conservative terms and normal form analysis to the Swift-Hohenberg equation by using multiple-scale methods. In addition, we also investigate Hamiltonian-Hopf bifurcations of two equilibria, crisis-cross snakes of one pulse and snaking bifurcation of two-pulse by numerical simulations. As for the snaking curve of N-pulse, we are also interested in it, and expect that N-pulses with $N \geq 3$ behave in a similar fashion. Especially, when a system presents a curve of isolas, how about the dynamics of the new system if we add two perturbed terms to Swift-Hohenberg equations? we will explore it in the near future work.

References

[1] M. Beck, J. Knobloch, D.J.B. Lloyd, B. Sandstede and T. Wagenknecht, Snakes, ladders, and isolas of localized patterns, *SIAM J. Math. Anal.*, **41**(2009),936-972.

[2] J. Burke, S.M. Houghton and E. Knobloch, Swift-Hohenberg equation with broken symmetry, *Phys. Rev. E*, **80**(2009),036202.

[3] A.R. Champneys, V. Kirk, E. Knobloch, B.E. Oldeman and J.D.M. Rademacher, Unfolding a tangent equilibrium-to-periodic heteroclinic cycle, *SIAM J. Appl. Dyn. Syst.*, **8**(2009),1261-1304.

[4] S.J. Chapman and G. Kozyreff, Exponential asymptotics of localised patterns and snaking bifurcation diagrams, *Physica D*, **238**(2009),319-354.

[5] P. Coullet, C. Riera and C. Tresser, Stable static localized structures in one dimension, *Phys. Rev. Lett.*, **84**(2000),3069-3072.

[6] J.H.P. Dawes, The emergence of a coherent structure for coherent structures: localized states in nonlinear systems, *Phil. Trans. R. Soc. A*, **368**(2010),3519-3534.

[7] E.J. Doedel and B.E. Oldeman, AUTO-07P: Continuation and bifurcation software for ordinary differential equations, Technical report, Concordia University, 2009.

[8] S.F. Deng, X.P. Li, Generalized homoclinic solutions for the Swift-Hohenberg equation, *J. Math. Anal. Appl.*, **390**(2012),15-26.

[9] E. Knobloch, Spatially localized structures in dissipative systems: open problems, *Nonlinearity*, **21**(2008),T45-T60.

[10] J. Knobloch, D.J.B. Lloyd, B. Sandstede and T. Wagenknecht, Isolas of 2-pulse solutions in homoclinic snaking scenarios, *J. Dynam. Diff. Eqns.*, **23**(2011),93-114.

[11] J. Knobloch, T. Rieß and M. Vielitz, Nonreversible homoclinic snaking, *Dynamical Systems*, **26**(2011),335-365.

[12] J. Knobloch, M. Vielitz and T. Wagenknecht, Nonreversible perturbations of homoclinic snaking scenarios, *Nonlinearity*, **25**(2012),3469-3485.

[13] G. Kozyreff and S.J. Chapman, Asymptotics of large bound states of localised structures, *Phys. Rev. Lett.*, **97**(2006),044502.

[14] J.D.M. Rademacher, Homoclinic orbits near heteroclinic cycles with one equilibrium and one periodic orbit, *J. Diff. Eqns.*, **218**(2005),390-443.

[15] J.D.M. Rademacher, Lyapunov-Schmidt reduction for unfolding heteroclinic networks of equilibria and periodic orbits with tangencies, *J. Diff. Eqns.*, **249**(2010),305-348.

[16] P.D. Woods and A.R. Champneys, Heteroclinic tangles and homoclinic snaking in the unfolding of a degenerate reversible Hamiltonian Hopf bifurcation, *Physica D*, **129**(1999),147-170.

[17] Uwe Thiele, Andrew J. Archer, and Mark J. Robbins, Localized states in the conserved Swift-Hohenberg equation with cubic nonlinearity, *Phys. Rev. E*, **87**(2013),042915.

[18] Y.C. Xu and T.Z. Lan, Localized patterns of the cubic-quintic Swift-Hohenberg equations with two symmetry-breaking terms, 2016. (In preparation)

[19] B. Sandstede, Y.C. Xu, Snakes and isolas in non-reversible conservative systems, *Dynamical Systems*, **27**(2012),317-329.

[20] J. Burke, E. Knobloch, Normal form for spatial dynamics in the Swift-hohenberg equation, *Discrete and Continous Dynamical Systems*, **87**(2007),170-180.

[21] J. Burke, and J.H.P. Dawes, Localized states in the Swift-Hohenberg equation, *SIAM J. Appl. Dyn. Syst.*, **11**(2012)261-284.

[22] Q.K. Xiao, H.J. Gao, Bifurcation in the Swift-Hohenberg equation, *J. of Comp. and Nonlinear Dyn.*, **11**:3(2016),031002.

(*edited by Mengxin He*)